Title:

Allometric scaling strengthens the relationship between eDNA particle concentration and organism abundance in nature

Running title:

Allometry and eDNA particle concentration

Authors:

Yates, M.C*[a], Glaser, D.[b], Post, J.[b], Cristescu, M.E.[c], Fraser, D.J.[d], and Derry, A.M.[a]

[a]Université du Québec à Montréal, 201 avenue Président-Kennedy, Montréal, Québec, H2X 3Y7

[b]University of Calgary, 507 Campus Dr NW, Calgary, Alberta, T2N 4V8

[c]McGill University, 1205 Dr Penfield Ave, Montreal, Quebec, H3A 1B1

[d]Concordia University, 7141 Sherbrooke St W, Montreal, Quebec, H4B 1R6

*Corresponding author: matthew.yates@outlook.com (514-919-5613)

Abstract

Organism abundance is a critical parameter in ecology, but its estimation is often challenging. Approaches utilizing eDNA to indirectly estimate abundance have recently generated substantial interest. However, preliminary correlations observed between eDNA concentration and abundance in nature are typically moderate in strength with significant unexplained variation. Here we apply a novel approach to integrate allometric scaling coefficients into models of eDNA concentration and organism abundance. We hypothesize that eDNA particle production scales non-linearly with mass, with scaling coefficients < 1. Wild populations often exhibit substantial variation in individual body size distributions; we therefore predict that the distribution of mass across individuals within a population will influence population-level eDNA production rates. To test our hypothesis, we collected standardized body size distribution and mark-recapture abundance data using whole-lake experiments involving nine populations of brook trout. We correlated eDNA concentration with three metrics of abundance: density (individuals/ha), biomass (kg/ha), and allometrically scaled mass (ASM) ($\sum$(individual mass$^{0.73}$)/ha). Density and biomass were both significantly positively correlated with eDNA concentration (adj. R^2 = 0.59 and 0.63, respectively), but ASM exhibited improved model fit (adj. R^2 = 0.78). We also demonstrate how estimates of ASM derived from eDNA samples in 'unknown' systems can be converted to biomass or density estimates with additional size structure data. Future experiments should empirically validate allometric scaling coefficients for eDNA production, particularly where substantial intraspecific size distribution variation exists. Incorporating allometric scaling may improve predictive models to the extent that eDNA concentration may become a reliable indicator of abundance in nature.

40 Keywords:

41 environmental DNA, eDNA, Abundance, Density, Biomass, Allometry, Allometric scaling

Introduction

Developing methods to estimate animal abundance in nature has attracted the attention of researchers and managers alike for over a century (Schwarz & Seber, 1999). Abundance is a fundamental population parameter in ecology, conservation, and natural resource management (Luikart, Ryman, Tallmon, Schwartz, & Allendorf, 2010), with direct impacts on ecological interactions (Krebs, 2009), ecosystem functioning (Schaus et al., 2010), population persistence and adaptability (Jamieson & Allendorf, 2012), as well as ecosystem services/resources (Immell & Anthony, 2008; Schwarz & Seber, 1999). Methodologies to estimate animal abundance represent a well-developed field of empirical research in ecology that has progressed remarkably (Schwarz & Seber, 1999; Seber, 1986). Yet despite this success, the estimation of abundance in nature is often challenging; obtaining robust estimates in natural populations using traditional methods can be time-consuming, costly, labor intensive, or even impossible to obtain for some populations (Luikart et al., 2010; Ovenden et al., 2016; Yates, Bernos, & Fraser, 2017).

The recent development of novel molecular tools has renewed interest in utilizing genetic information to indirectly estimate abundance in difficult-to-sample natural populations (Goldberg, Strickler, & Pilliod, 2015; Luikart et al., 2010). Molecular techniques that quantify the concentration of environmental DNA (eDNA) particles represent a promising tool, with recent studies demonstrating support for a correlation between eDNA concentration and abundance (Pilliod, Goldberg, Arkle, & Waits, 2013; Takahara, Minamoto, Yamanaka, Doi, & Kawabata, 2012; Thomsen et al., 2012). For example, laboratory studies have demonstrated a strong correlation between eDNA concentration and abundance (Eichmiller, Miller, & Sorensen, 2016; Klymus, Richter, Chapman, & Paukert, 2015), exhibiting a mean correlation coefficient of 0.9 ($R^2 = 0.81$) (Yates, Fraser, & Derry, 2019). Studies in nature, however, have generally found

65 weaker correlations than laboratory studies, with a mean correlation coefficient of 0.71-0.75 (R^2
66 = 0.51-0.57) (Yates et al., 2019). Although correlations remain moderately strong in nature,
67 much of the variation in eDNA particle concentration across environments often remains
68 unexplained. As a result, the extent to which eDNA could be used to reliably infer abundance in
69 nature remains limited without significant improvements in modelling or technology.
70 In nature, organismal abundance is typically quantified by evaluating individual density
71 (i.e. individuals/unit area) or biomass density (i.e. kg/unit area). While both metrics of abundance
72 appear to correlate equally well with species-specific eDNA particle concentration in the wild,
73 processes involved in the production of eDNA particles in natural environments are unlikely to
74 scale linearly with either biomass or density. Although eDNA production tends to increase with
75 individual mass (Maruyama, Nakamura, Yamanaka, Kondoh, & Minamoto, 2014), individuals
76 with a large biomass often produce fewer eDNA particles than equivalent biomass of smaller
77 conspecifics (Maruyama et al., 2014; Mizumoto, Urabe, Kanbe, Fukushima, & Araki, 2017;
78 Takeuchi, Iijima, Kakuzen, Watanab, & Yamada, 2019). As such, eDNA particle concentration
79 would be expected to vary, for example, between environments that contain equal densities of
80 individuals but with varying biomass. Similarly, environments with equal biomass but varying
81 densities would also be likely to vary in observed eDNA particle concentration. Wild populations
82 often exhibit substantial inter-population variation in the distribution of individual biomass
83 (Donald, Anderson, Mayhood, Anderson, & Correlations, 1980; Guernon, Yates, Fraser, &
84 Derry, 2018; Millien et al., 2006; Sebens, 1987), which may in turn scale to affect overall
85 population-level rates of eDNA production (Maruyama et al., 2014) and partially account for the
86 substantial unexplained variation observed between eDNA concentration and traditional metrics
87 of abundance (e.g. density and biomass) in nature (Yates et al., 2019).

Here, we extend models of physiological allometric scaling to organismal eDNA particle production to provide a framework through which differences in density, total biomass, and the distribution of individual biomass can be integrated into models of eDNA production in natural populations. Excretory processes (urine, fecal matter, etc.) and shedding (from scales, skin, mucous, etc.) are thought to be the two major physiological processes that contribute to the production of eDNA particles (Jo, Murakami, Yamamoto, Masuda, & Minamoto, 2019; Stewart, 2019). The metabolic theory of ecology (MTE) provides a robust, empirically validated framework through which allometry in metabolic processes (including excretion) can be modelled. The MTE posits that metabolic processes scale non-linearly with body size according to the power function:

$$I = I_0 * M^b$$

where I = metabolic rate, I_0 = a normalization constant, M = organism body mass, and ^{b} = an allometric scaling coefficient (Allegier, Wenger, Rosemond, Schindler, & Layman, 2015; Brown, Gillooly, Allen, Savage, & West, 2004; Vanni & McIntyre, 2016). The value of b varies depending on the physiological process; metabolic rates typically scale to the power of 0.75 (Brown et al., 2004; Isaac & Carbone, 2010), whereas values for consumptive or excretory rates are often lower (Post, Parkinson, & Johnston, 1999; Vanni & McIntyre, 2016). Nevertheless, metabolic theory predicts that larger organisms tend to exhibit disproportionately lower rates (relative to their mass) for metabolically linked processes such as excretion (Allen & Gillooly, 2009; Vanni & McIntyre, 2016). While shedding from mucous, scales, or skin may also be linked to metabolic rates, shedding rates are also likely a function of the surface area of an organism. In many aquatic organisms (particularly fish) the allometric relationship between body mass and surface area follows a similar mathematical form as metabolic processes; salmonids,

for example, exhibit mass-scaling coefficients for surface area between 0.59 and 0.65 (Shea, Fryer, Pert, & Bricknell, 2006).

Metabolic rates, excretory rates, and surface area (via shedding) are likely to collectively impact eDNA production, yet all follow a similar allometric form; as a result, we hypothesize that eDNA production can also be modelled as a power function of individual mass and an exponential scaling coefficient with a value less than 1. This hypothesis has important consequences for ecosystem-level processes; the utility of integrating allometric scaling in ecosystem-level models of ecological stoichiometry (Allen & Gillooly, 2009), animal excretion (Vanni & McIntyre, 2016), consumption (Post et al., 1999), and nutrient cycling (Schaus et al., 2010; Schindler & Eby, 1997), for example, has long been acknowledged with broad empirical support. We therefore further hypothesize that, when scaled to the level of an entire population, allometric scaling in eDNA production will also have a substantial effect on overall population-level production of eDNA. We consequently predict that the incorporation of mass scaling coefficients to account for inter-population variation in density, biomass, and the distribution of biomass across individuals will improve modelling efforts linking eDNA particle concentration and abundance across natural ecosystems.

To test our hypothesis, we collected standardized individual biomass data and used classic mark-recapture experiments to enumerate abundance in nine populations of brook trout in the Rocky Mountains of Canada while simultaneously collecting eDNA samples in each lake. Study populations exhibited substantial variation in individual density (63 - 1177 individuals/ha), biomass density (12.6 - 52.4 kg/ha), and mean body size (43.0 - 405.9 g/individual). We applied these data to specifically test two key predictions: i) brook trout eDNA particle concentration will correlate with traditional metrics of abundance (density and biomass) across the nine study

134 lakes; and ii) incorporating allometric scaling coefficients to estimates of brook trout abundance
135 (e.g. $\sum$(individual biomass$^{0.73}$)/ha, or "allometrically scaled mass" (ASM)) will substantially
136 improve models of abundance and eDNA particle concentration.

137 ASM estimates derived from known eDNA concentrations in novel systems lacking
138 abundance data cannot be directly converted to traditional metrics of abundance (e.g. density and
139 biomass) because multiple density/biomass configurations (e.g. many small fish or a small
140 number of large fish) can produce equivalent ASM values. However, using a real-world
141 example, we also demonstrate how ASM estimates derived from known eDNA concentrations
142 for systems that lack abundance data on a target species can be converted into traditional
143 estimates of abundance with additional size structure data.

Materials and Methods

Study species and system

Nine brook trout populations introduced in the early 20th century to lakes located in Kootenay, Banff, and Yoho national parks (Figure S1) were monitored to determine population size (number of individuals > 80mm) and individual biomass distributions. Study populations experience little recreational fishing pressure due to no-take policies implemented within the National Parks.

Mark-recapture surveys and size structure estimates

Mark-recapture studies were conducted in 2018 between May 27th and June 30th, except for Cobb lake where isolated marking events occurred until September 12th (Figure S2). Fish were captured using a combination of fyke nets, angling, and backpack electrofishing (Table 1). Large (1 m hoop diameter, 2 cm mesh) and small (0.7 m hoop diameter and 0.8 cm mesh) fyke nets were distributed around the perimeter of lakes with the lead attached to shore and the end of the trap facing the center of the lake. Nets were checked daily to reduce stress to fish and possible cannibalism. Angling was used to supplement fish capture efforts at sites where fyke catchability was low (predominantly Cobb). Marks were also assigned to fish captured by electrofishing the shore and inlets/outlets of lakes with a backpack electrofisher (Smith-Root, Vancouver, Washington, USA)

Captured fish were anesthetized using clove oil and measured for fork length (± 1mm) and mass (± 0.1g). Any unmarked fish were gastrically tagged with a BioMark HPT8 pre-loaded Passive Integrated Transponder (PIT) tag (Boise, Idaho, USA). Only fish greater than or equal to 80 mm were tagged to reduce tagging mortality. The tag number of any recaptured fish was

167 recorded. All fish were processed in the shade with aerators to avoid unnecessary stress.
168 Recovered fish were released in the center of the lake to standardize release location and
169 promote mixing (e.g. if released near shore, fish may have been recaptured in an adjacent net,
170 biasing mark recapture data). Marking ceased once recapture ratios approached twenty five
171 percent for several consecutive days.

172 Size structure estimates aimed to obtain a representative snapshot of the size structure of
173 each population and was conducted between July 27th and September 1st, with the exception of
174 Cobb where size structure assessments continued to October 12th (Figure S2). Fish were captured
175 in large and small sinking mixed mesh gillnets with clear monofilament. Large mixed-mesh
176 gillnets were 15.6 m long, 1.8 m deep and had an equal area of 64-51-89-38-76 mm mesh panels.
177 Small mixed-mesh gillnets were 12.5 meters long, 1.8 meters deep, and consisted of an equal
178 area of 32-19-38-13-25 mm mesh panels. Index nets are widely used in North America for size
179 structure assessments (Bonar, Hubert, & Willis, 2009; Hubert, Pope, & Dettmers, 2012; Johnson,
180 1983; Post et al., 1999; Ward, Askey, Post, Varkey, & Mcallister, 2012) as these attempt to
181 capture a representative size/age structure of the population (Morgan, 2002). Nets were checked
182 daily and moved if they were being reset. Sampling ceased when approximately five to ten
183 percent of the population was captured, apart from Cobb lake where size structure assessment
184 captured approximately 71% of individuals (Table 1). Captured fish were euthanized with clove
185 oil, PIT tags were recorded, and length/mass data were collected as described for the marking
186 period.
187

Population size estimation

Schnabel population size estimates, which utilize sequential marking/recapture events, were used to determine the number of fish in a lake (Schnabel, 1938). All size structure assessment removals were pooled together into one final sampling event for the population estimates which controlled for the removal of marks at large (*M*). Note that population estimates only account for fish greater the minimum tagging size (80 mm fork length). All population estimates were conducted in R (R Development Core Team, 2017) with the *mrClosed* function from the Fisheries Stock Assessment package FSA (Ogle, 2016). Confidence intervals for Schnabel population estimates followed recommendations from (Seber, 2002) as implemented in the FSA package.

Density calculation

To link eDNA particle concentration with fish abundance, three metrics of density were calculated: (i) individual density (individuals/ha); (ii) biomass density (biomass/ha); (iii) and allometrically scaled mass (ASM/ha). Individual density was estimated by dividing the population size estimate by lake size (ha). Biomass density was calculated according to the following formula:

$$biomass\ per\ ha = \frac{\frac{\sum_{i=1}^{N_{SA}} mass_{SA}}{N_{SA}} \cdot \widehat{N}}{area\ (ha.)}$$

Where $\sum_{i=1}^{N_{SA}} Mass_{SA}$ is the sum of the masses captured in the index net during size structure assessment, N_{SA} is the number of fish captured in the index nets, $\widehat{N}$ is the estimated population size. This methodology assumes that the size structure assessment was representative of the population.

ASM was calculated by replacing the mass measure with $mass^{0.73}$ according to the

210 formula:

211 $$ASM\ per\ ha = \frac{\frac{\sum_{i=1}^{N_{SA}}(mass_{SA}^{0.73})}{N_{SA}} \cdot \widehat{N}}{area\ (ha.)}$$

212

213 This density metric was included to account for the relative decline in mass-specific eDNA
214 production or excretion rates typically observed as individual organismal mass increases
215 (Maruyama et al., 2014; Takeuchi et al., 2019; Vanni & McIntyre, 2016). Scaling coefficients
216 can vary substantially depending on the physiological process, taxonomy or environment
217 (Allegier et al., 2015; Glazier, 2005). In the absence of data on allometric scaling in eDNA
218 production, data on allometric scaling in metabolic or excretory rates for the same study species
219 can represent useful starting points. Data on allometry in excretory rates were unavailable for
220 brook trout, so the metabolic scaling coefficient obtained from (Hartman & Cox, 2008) was
221 used: data extracted using the R package *digitizer* (Poisot, 2011) and back-transformed from
222 figure one in (Hartman & Cox, 2008) indicate an allometric metabolic scaling factor of
223 approximately 0.73 (0.03 SE).

224 In difficult to sample populations, estimates of relative abundance are often obtained
225 using CPUE metrics. As a result, most previous studies examining eDNA particle concentration
226 and abundance utilize similar metrics (Yates et al., 2019). To evaluate the utility of CPUE as a
227 'proxy' metric of abundance in our study system, CPUE for each lake was quantified as the
228 mean catch per-unit effort of a large and small index gillnet.

229

eDNA sample collection

eDNA samples were collected between June 30 and July 13th, 2018. Sampling was equidistantly distributed around each lake and included four littoral and four pelagic samples. Littoral samples were collected approximately 1-3 m from shore at a depth of least 12 inches but six inches above the bottom to avoid the unintentional collection of sediments. Pelagic samples were collected from each lake by drawing a line through the center of the lake along its longest axis; samples were collected along this axis at equidistant intervals at a depth of approximately 0.5m. To avoid between-lake contamination all eDNA samples were collected either from an inflatable kayak that was decontaminated 48h prior in a 2% bleach solution for 15 minutes (including paddle and life-jacket) or from a canoe assigned to sample a single specific lake. Water samples were collected using sterile Whirl-Pak™ bags (Uline, Ontario, Canada).

Samples were immediately filtered on the lakeshore using two chlorophyll filtering manifolds bleached in a 30% household bleach solution for ten minutes 2-12h prior to collection. All samples were stored in the shade prior to filtration in plastic washbasins bleached with a 30% solution for ten minutes, and all filtering was conducted in the shade under a tarp. Manifolds were transported in a Polar Bear™ backpack cooler (Polar Bear Coolers, Georgia, USA) whose interior was wiped with a 30% bleach solution for ten minutes. Manifold components were stored after bleaching and transported individually in sealed plastic zippered bags to limit contamination. Pencils and markers were also wiped with a 30% bleach solution.

One L of sample water from each site was filtered through a 0.7µm-pore glass fibre filter (GE Healthcare Life Sciences, Ontario, Canada) using a vacuum hand pump (Soil Moisture, California, USA); each vacuum pump was decontaminated between lakes by wiping with a 30% bleach solution and resting for ten minutes. All littoral samples were filtered on one manifold

and all pelagic samples were filtered on the other. Prior to filtering lake water samples, 1 L of distilled water was filtered through each manifold as a negative control. Filters were handled using two metal forceps bleached in a 30% solution for ten minutes and transported in individual bags; one forceps was used for littoral samples and another forceps was used for pelagic samples. After filtering, filters were folded and placed directly in a sterile 2 ml microcentrifuge tube filled with 700µl AL buffer (Qiagen, Maryland, USA) which was then labelled and individually sealed in a plastic zippered bag and placed in a 2nd cooler that was decontaminated by wiping with a 30% bleach solution and resting for ten minutes. This cooler contained two frozen freezer-gel packs decontaminated in a 30% bleach solution for ten minutes. If a filter became clogged (i.e. < 1 L of water was filtered) the final volume of water filtered was recorded and the sample was stored in buffer. Filters were immediately transported to and stored in a -20 ℃ freezer (wiped with 30% bleach and soaked for ten minutes) at Kootenay Crossing. Filters were stored on dry ice for transportation to Montreal where they were stored in a -80 ℃ freezer.

eDNA extraction and analysis

Each filter was extracted using a Qiagen DNeasy Blood and Tissue ^{TM} kit and Qiashdredder^{TM} spin column following a modified extraction protocol (see Appendix S1 for details). Final DNA product was eluted into 130 µl of AE buffer and stored in a clean -20 ℃ freezer dedicated to the sole storage of eDNA samples. To avoid cross-contamination between lakes extractions were conducted on batches from a single lake, with a single extraction blank of 700 µL AL buffer included as an extraction control. Decontamination procedures were identical for both manifolds, so only a single negative control was extracted per lake. All extractions were conducted in an extraction room dedicated to the handling of sensitive eDNA samples. This room receives weekly cleaning with a 10% bleach solution and is free of PCR products or high-

concentration DNA. All individuals entering the extraction room were required to wear nitrile gloves, hair nets, shoe covers, and dedicated, clean lab coats. All lab surfaces were soaked with a 20% bleach solution for ten minutes before and after extractions. PCR Clean Wipes™ (Thermo Scientific, Massachusetts, USA) were also used to decontaminate all lab surfaces and pipettes prior to and after extracting or handling eDNA samples.

The concentration of brook trout eDNA was quantified using the TaqMan minor groove assay published in (Wilcox et al., 2013), which targets a region of the brook trout cytochrome *b* mitochondrial gene. All samples were run in triplicate at a 20 µl final reaction volume on a Stratagene MX 3000P thermal cycler using Environmental Master Mix 2.0 and 5 µl of template DNA. Forward and reverse primers were included at a final concentration of 900 nM, with the probe at a final concentration of 250 nM. Each replicate was spiked with an internal positive control to test for inhibition; any replicate that exhibited inhibition ($Ct > 1$ in the internal positive control) was reanalyzed with diluted template DNA at 60% concentration (3 µl template + 2 µl of ultrapure water); this was sufficient to relieve inhibition in all cases. Standard curve template DNA was composed of a synthetic Gblock™ gene fragment (IDT, Iowa, USA) of the targeted sequence. A triplicate no template control and triplicate five-point standard curve (1250 copies/µl, 250 copies/µl, 50 copies/µl, 5 copies/µl, 2 copies/µl template concentration) were included on each 96-well plate. All qPCR reaction reagents were aliquoted into single-use volumes adequate for a single plate and reactions were prepared in the dedicated eDNA room, with the exception of the standard curve replicates due to the presence of high concentration synthetic DNA fragments. Reactions were cycled with an initial hold at 95 °C for ten minutes followed by 45 cycles of 30 seconds at 95 °C and 1 min at 60 °C. eDNA particle concentration at each site was determined by averaging site-specific replicates. Final mean copy number values

were converted (based on total volume of water filtered per sample) to total eDNA particle concentration per 1 L of sampled water (copies/L).

Data Analysis

Mean eDNA particle concentration (copies/L) for each lake was calculated by first averaging eDNA particle concentrations of the four littoral and four pelagic samples to obtain mean littoral eDNA concentration and mean pelagic eDNA concentration. The surface area of a (roughly) circular object increases non-linearly in relation to perimeter and, as a result, the area of the pelagic zone expressed as a fraction of the total area of a lake tends to increase with lake size. The relative contribution of the littoral and pelagic zones to the overall mean concentration of eDNA per lake should therefore be increasingly weighted towards the pelagic eDNA concentration as lake surface area increases. Our study lakes varied substantially in size (1.7 to 18.5 ha); total pelagic and littoral areas were calculated for each lake using polygons on Google Earth. In the absence of detailed bathymetry data, the total area of the littoral zone was calculated by including all lake surface area up to 20m from the shore, with the remaining area assigned to the pelagic zone. A weighted-mean eDNA concentration for each lake was then calculated by weighing the littoral and pelagic eDNA concentrations based on the fraction of total lake area each zone represented.

Mean lake eDNA particle concentration (copies/L) was modelled separately as a function of the three metrics of brook trout density calculated above: individual density (individuals/ha); biomass density (kg/ha); and allometrically scaled mass (ASM) ($\sum$(individual mass$^{0.73}$)/ha). eDNA particle concentration was included as a dependent variable in a linear regression and a separate model for each abundance metric was fitted to the observed data. Wald *F*–tests were used to evaluate the significance of fixed-effect terms, with AIC (Akaike, 1974) values used to

compare model fit as in (Lacoursière-Roussel, Côté, Leclerc, Bernatchez, & Cadotte, 2016). All analyses were conducted in R (v.3.3.3) (R Development Core Team, 2017). To assess the performance of CPUE as a 'proxy' metric of abundance, we also examined the relationship between density and CPUE, as well as eDNA particle concentration and CPUE, using linear regression.

Estimating density and biomass from predicted allometrically scaled mass: a case study for population management

Most researchers/managers would be primarily interested in predicting traditional metrics of abundance (i.e. density and biomass) from estimated eDNA particle concentrations in similar ecosystems that lack abundance data. Predicting abundance in unknown systems from known eDNA particle concentrations would require an inversion of the modelling relationship described above: abundance would be modelled as a function of eDNA particle concentration. Predicted estimates of ASM obtained from eDNA samples collected for systems lacking abundance data cannot be directly converted to traditional metrics of abundance (e.g. individual density or biomass density) because multiple density/biomass configurations (e.g. many small fish or a small number of large fish) can produce equivalent ASM values. However, predicted ASM point-estimates for a system with unknown abundance can be converted to traditional metrics with additional individual mass distribution data from standardized size structure data. Size structure data from the unknown system could be scaled allometrically and the resulting scaled mass values nonparametrically bootstrapped (with replacement) until the cumulative sum of the bootstrapped values equals the predicted ASM. Individual density could be estimated by totalling the number of bootstrap "samples" summed to achieve the predicted ASM; biomass density

could then be estimated by multiplying the predicted density value by the untransformed mean of the individual biomass distribution.

As a case study, this technique was applied to data collected from Hidden Lake (Banff, Alberta, Canada). The brook trout population of Hidden Lake was targeted as part of rotenone-based removal program by Parks Canada. eDNA samples from Hidden lake were collected in July 2018 and extracted/analyzed using the same methodology as described above. The estimated "ASM/unit area" of the lake (including 95% prediction intervals) was calculated from the linear relationship obtained from our nine study lakes. Unfortunately, standardized size structure data were unavailable; rotenone removal efforts began in August 2018 and no brook trout remain in the system. However, prior to the use of rotenone mechanical gill netting efforts were employed during brook trout removal efforts between 2011 and August 2017 (Stitt, *perse. comm.*). By 2016 netting efforts had removed most large fish from the population. Most netted fish older than age 0+ in Hidden lake were therefore between 90-140mm in length (Sullivan, Sierra, 2017), although it should be noted that size distribution data obtained from these netting efforts were not directly comparable to our standardized size structure assessments due to different netting methodology/gear. The size distribution of fish removed by Parks Canada in 2016 most closely resembles the size distribution of fish in Olive lake, so the Olive size distribution was utilized as a "proxy" to calculate an approximate pre-rotenone individual density and biomass density of brook trout inhabiting Hidden lake in 2018. The size distribution of fish from Olive lake is slightly larger (mean = 149mm) than the 2016 Hidden lake distribution; as a result, population size estimates derived from this distribution will likely slightly underestimate the 'true' number of individuals present in Hidden Lake. Bootstrap simulations to quantify individual density and biomass density utilizing the Olive size distribution and predicted ASM of

368 Hidden lake were run for 1000 iterations. Parks Canada estimated the 2018 pre-rotenone
369 population of Hidden Lake to be between 3300 and 5000 individuals based on the retrieval of
370 fish corpses post-rotenone, providing some degree of external validation for our predictive model
371 (Stitt, B, 2018).

372 *Predicting allometric scaling coefficient for eDNA production in brook trout*

373 Allometric scaling coefficients are likely to fall between a value of 0.0 and 1.0; notably,
374 ($\sum$ individual mass$^{0.0}$)/ha is equivalent to individual density (fish/ha) and ($\sum$individual
375 mass$^{1.0}$)/ha is equivalent to biomass density (kg/ha). Although we employed an allometric scaling
376 coefficient of 0.73 in our model (based on metabolic data from brook trout), the "true" allometric
377 scaling coefficient for eDNA production in our system was unknown. We used our data to
378 predict the optimal value for the scaling coefficient given the observed eDNA particle
379 concentration and biomass distribution data observed across our study lakes. To achieve this, we
380 iteratively generated ASM values from our data using scaling coefficients ranging from 0.00 to
381 1.00 (increasing by intervals of 0.01) and sequentially modelled eDNA particle concentration
382 data as a function of each ASM value. AIC values for each model were then used to evaluate
383 model fit. If eDNA production scales allometrically according to a power function, we predict
384 that the AIC values across models with scaling coefficients between 0.0 and 1.00 will exhibit an
385 approximately upward parabolic distribution with a minimum best-fit value that corresponds to
386 an "optimal" allometric scaling coefficient. According to the general rule described in (Burnham
387 & Anderson, 2002), models with AIC values within 2 units of the best-fit model AIC (e.g. ΔAIC
388 < 2) also exhibit substantial support; we predict that the 'true' allometric scaling coefficient for
389 brook trout eDNA production in nature will fall between the range of scaling coefficients that

produce models within 2 AIC of the 'best-fit' scaling coefficient, although future experiments will be necessary to validate our predictions.

Results

Population size estimates and density

Population size estimates ranged from 145 to 3266 individuals, individual density ranged from 63 to 1131 fish/ha, biomass density ranged from 12.6 to 52.5 kg/ha, and ASM ranged from 3707 to 18600 ASM/ha (Table 2, see Figure 1 for population size structure). Estimates of catch-per-unit-effort (CPUE) did not exhibit a significant correlation with individual density ($F_{1,7}$ = 0.53, p = 0.491, Figure S3).

eDNA concentrations and correlations with density metrics among lakes

Brook trout eDNA was successfully amplified from all samples in all lakes. No amplification was observed in any negative controls or extraction blanks. The R^2 values for standard curves ranged from 0.984 to 0.995, with an estimated efficiency ranging from 84.2 to 95.1%. Littoral and pelagic eDNA concentrations varied substantially by lake (Table 3). After weighing for lake zone area, mean eDNA concentrations ranged from 592 copies/L in Cobb to 7805 copies/L in Olive.

Linear models for each density metric demonstrated positive and significant correlations with eDNA particle concentration (Table 4, Figure 2). Individual density, biomass density, and ASM accounted for 59%, 63%, and 78% of the variation in observed eDNA particle concentration (adjusted R^2), respectively. AIC values indicated that individual density and biomass density metrics provided roughly equivalent model fit; however, the ASM metric provided substantially improved model fit relative to individual density and biomass density (ΔAIC of 5.7 and 4.6, respectively). CPUE did not exhibit a significant correlation with eDNA particle concentration (Table 4, Figure S4).

Estimating density and biomass from predicted allometrically scaled mass: a case study for population management

The eDNA concentration of Hidden lake littoral and pelagic eDNA samples averaged 2653 and 342 copies/L, respectively, with a weighted mean average eDNA particle concentration of 847 copies/L (Table 3). Based on a linear model using data from the nine study lakes, Hidden lake had an estimated ASM/ha of 4279.6 (Figure 3). The predicted ASM estimate for Hidden Lake was converted to traditional metrics of abundance (individual density and biomass density) by bootstrap sampling allometrically scaled mass values (with replacement) from the Olive lake size structure distribution (which was closest to the likely size structure of the Hidden lake population) until the cumulative sum of all bootstrap sampled values equalled the predicted ASM/ha from the linear model. After 1000 iterations, the mean number of individual mass values sampled from the Olive size distribution was 278.4, which represents the individual density (ind/ha) point-estimate for Hidden Lake; this corresponds to a total population size estimate of 3286 individuals. This point estimate was similar to the 2018 pre-rotenone population size estimate from Parks Canada of 3300-5000 individuals (Stitt, B, 2018), given the use of the slightly larger Olive size distribution during the bootstrap procedure. Predicted total biomass was 143.0 kg, with a biomass density of 12.1 kg/ha. Notably, point estimates of biomass density rank Hidden lower than all nine study lakes, likely as a result of previous fish removal efforts between 2011 and 2017 in Hidden Lake. Upper 95% prediction intervals for population size, total biomass, density, and biomass were 7629 individuals, 332.0 kg, 646.5 fish/ha, and 28.1 kg/ha, respectively. Due to the overall low concentration of eDNA present in the lake lower 95% prediction intervals overlapped with zero for all four parameters.

438 *Predicting the allometric scaling coefficient for eDNA production in brook trout*

439 Based on model AIC values, a scaling coefficient of 0.72 best explained patterns of

440 eDNA particle concentration across the nine study lakes; models with scaling coefficients

441 between 0.47 and 0.89 generated ΔAIC values < 2 (Figure 4).

Discussion

Our study provides strong support for the hypothesis that eDNA production scales non-linearly with mass according to a power function. Incorporating allometric scaling coefficients to account for the distribution of biomass across individuals substantially improved predictive models, indicating that the distribution of biomass across individuals within a population may have an important effect when scaling individual eDNA production rates to the population-level. Incorporating metabolic scaling coefficients for mass into models of eDNA particle concentration and organismal abundance may therefore be particularly important in species that exhibit substantial inter-population variation in size distributions. Our findings contribute to a broader understanding of the ecology of eDNA production and have important implications for many eDNA applications. While the focus of this study was on the relationship between eDNA particle concentration and abundance using qPCR techniques, allometry in species with variable size structure could, for example, partially account for the variation observed in species-specific read number across environments in metabarcoding studies.

This study also reaffirms previous findings that metrics of population abundance correlate with species-specific eDNA particle concentration in natural environments (Klobucar, Rodgers, & Budy, 2017; Nevers et al., 2018; Pilliod et al., 2013; Schmelzle & Kinziger, 2016; Thomsen et al., 2012). Previous research has demonstrated a moderate correlation between density and/or biomass and eDNA particle concentration in lotic systems for brook trout (Baldigo, Sporn, George, & Ball, 2017; Wilcox et al., 2016). We found similar relationships within lentic systems, but also demonstrate that they can be considerably improved by integrating allometric scaling coefficients into estimates of organismal abundance.

Notably, the correlation coefficients we observed between eDNA concentration and all three metrics of abundance were greater than most previous studies conducted in nature (Yates et al., 2019). The relatively strong correlations we observed between our abundance metrics and eDNA concentration could also be due to the methodology with which we assessed population size. Our estimates of population size were obtained using mark-recapture studies and unbiased measures of size-structuring, which provided precise and standardized estimates of individual density, biomass density, and ASM. However, such estimates are rare in published eDNA/abundance studies; conducting mark-recapture studies to estimate population size are time consuming and require a substantial commitment of labour and resources. To date only a handful of eDNA studies in nature have specifically enumerated population size (Klobucar et al., 2017; Levi et al., 2019; Tillotson et al., 2018) rather than proxies for abundance, such as CPUE (Yates et al., 2019). CPUE may be appropriate if it exhibits a strong correlation with abundance, but in some systems CPUE can perform poorly as a proxy for abundance (Hubert et al., 2012; Rose & Kulka, 1999). In our study systems CPUE did not exhibit a significant correlation with individual density and, as a result, eDNA concentration. Some of the substantial unexplained variation in nature between eDNA concentration and abundance observed in other systems could result from reliance on CPUE as a 'proxy' for abundance, although we acknowledge that for many species it may often be impractical or impossible to directly estimate population size.

It is important to note, however, that our abundance estimates may miss a small fraction of the adult population and do not account for juvenile (age 0+) abundance because fish were not included in the mark-recapture study until they were at least 80mm (to avoid excessive tagging mortality). Population size estimates therefore represent underestimates of true population census size. Discrepancies in juvenile abundance/density across lakes could account for some of the

487 remaining unexplained variation present in our model, particularly since smaller fish would be
488 expected to exhibit higher mass-specific eDNA production rates. Similarly, temperature is
489 known to have a strong effect on metabolic rates (Brown et al., 2004) and eDNA production (Jo
490 et al., 2019). Notably, Temple lake exhibited a substantially lower concentration of eDNA than
491 expected from its ASM estimate; at 3.5 ℃, Temple lake was also substantially colder than the
492 other eight study lakes during eDNA sampling (8.9-17.2 ℃). Although we lacked the replication
493 to do so, integrating other important environmental variables (e.g. temperature, pH, etc.) into
494 models of eDNA particle concentration across environments could further improve predictive
495 models.

496 Despite these caveats, we demonstrate that it is possible to predict estimates of abundance
497 with eDNA samples and population size structure data in similar ecosystems that lack abundance
498 data. The population size point estimate for Hidden Lake from our ASM/eDNA model (and
499 based on the Olive "proxy" size distribution) was similar to the pre-rotenone population size
500 based on Parks Canada estimates. Although predicted density metrics for Hidden lake exhibited
501 wide upper 95% prediction intervals, they still provided enough information to facilitate relative
502 comparisons to the nine study lakes; we can predict with some certainty, for example, that
503 Hidden Lake had a lower biomass density relative to two of the nine study lakes (Dog and
504 Olive). Furthermore, 95% prediction intervals represent a relatively stringent criteria of certainty;
505 75% or 80% prediction intervals might still represent "good enough" information to help guide
506 managerial or research decisions.

507 Most significantly, our results highlight the need for further empirical studies exploring
508 and validating allometric scaling via power functions as a framework for modelling eDNA
509 particle production rates. While we demonstrate that incorporating allometric scaling coefficients

510 substantially improves models predicting abundance and eDNA concentration at the population
511 level, we have not directly quantified how eDNA production scales allometrically in brook trout
512 at the level of individual organisms. Nevertheless, recent experiments demonstrate that mass-
513 specific eDNA production rates tend to decline as individual mass increases (Maruyama et al.,
514 2014; Mizumoto et al., 2017; Takeuchi et al., 2019). We found that a scaling coefficient of 0.72
515 best described patterns of eDNA concentration for our study species across our nine study lakes;
516 this value closely aligned with the metabolic scaling coefficient for brook trout from (Hartman &
517 Cox, 2008). Scaling coefficients between 0.51 and 0.87 produced models with ΔAIC values < 2;
518 we therefore predict that the 'true' allometric scaling coefficient for eDNA production in brook
519 trout will likely fall within this interval. To validate our findings and test our subsequent
520 predictions, further experiments to quantify allometric scaling of eDNA production at the
521 individual level in brook trout are necessary.

522 As a well-supported general theory in ecology, experimental designs developed to test
523 MTE hypotheses (e.g. (Allegier et al., 2015; Hartman & Cox, 2008)) can inform future
524 experiments examining the effect of allometry on eDNA production rates. Notably, previous
525 experiments investigating allometric scaling in excretion or metabolic rates quantified rates at the
526 level of *individual* organisms (Allegier et al., 2015; Hartman & Cox, 2008; Vanni & McIntyre,
527 2016). Previous laboratory experiments quantifying the effect of biomass on eDNA
528 production/shedding rates typically pooled organisms to create different biomass treatments
529 (Doi, Uchii, Takahara, & Matsuhashi, 2015; Klymus et al., 2015; Lacoursière-Roussel, Rosabal,
530 & Bernatchez, 2016; Mizumoto et al., 2017; Takahara et al., 2012). At best, such experiments
531 pool organisms from similar size-classes, in which case eDNA production/abundance
532 relationships across 'treatments' only reflect changes in abundance within a specific age- or size-

class. Such experimental designs are likely to produce a strong relationship between eDNA concentration and biomass, as has been found in a meta-analytic review (Yates et al., 2019). While such studies were necessary to empirically quantify a preliminary correlation between eDNA particle concentration and metrics of abundance, they might obscure critical differences in mass-specific eDNA production rates across size classes that could have important consequences for population-level rates. Natural populations often exhibit substantial variation in the distribution of body size across individuals; the failure to account for allometric scaling in the relationship between biomass and eDNA production might partially explain the failure to translate the strong relationships observed in laboratory experiments to nature (Sebens, 1987). Notably, our eDNA/abundance models utilizing ASM exhibited correlation coefficients comparable to those typically observed in laboratory environments (Yates et al., 2019).

It may be possible to investigate allometry in eDNA production by pooling individuals that are the same size within replicates. However, we would advise against this because behavioural interactions between fish at high density in confined spaces may impact eDNA production; some studies have demonstrated that eDNA production per fish increases at high densities (Id et al., 2019). Brook trout, for example, are known to exhibit aggressive behaviour towards conspecifics (McNicol, Scherer, & Murkin, 1985), which could increase eDNA particle concentration at high densities due to increased activity and/or injuries inflicted upon each other. If size classes exhibit different behaviour at high densities, this could further affect estimates of allometric scaling. Future studies examining allometric scaling in eDNA production should therefore incorporate individuals from a gradient of age/size classes and quantify organismal eDNA production at the *individual*-level, as in (Takeuchi et al., 2019). Notably, the two studies to examine eDNA production rates at an individual level across age/size classes found that

556 larger, older individuals exhibited lower mass-specific eDNA production rates (Maruyama et al.,
557 2014; Takeuchi et al., 2019). There is also a critical need to conduct such experiments *in situ* at
558 field study sites on wild organisms, as in (Pilliod, Goldberg, Arkle, & Waits, 2014). Laboratory
559 experiments, while important from a validation perspective, may not reflect natural excretion
560 processes because study organisms are housed in artificial conditions, fed artificial diets, and are
561 often subject to fasting regimes (Vanni & McIntyre, 2016). Furthermore, size-scaling
562 coefficients for metabolic processes such as nutrient excretion exhibit substantial interspecific
563 variation and can even include values greater than 1 (Allegier et al., 2015; Vanni & McIntyre,
564 2016). Allometric scaling in eDNA production may therefore exhibit similar variability across
565 species and should be investigated on a case-by-case basis.
566

567 *Conclusions*

568 Our results provide evidence supporting the hypothesis that eDNA production scales
569 allometrically with organism mass and can be modelled according to the power function:

570 $$I = I_0 * M^b$$

571 We have demonstrated that the incorporation of additional (but straightforward to collect) size
572 structure data to integrate key allometric scaling predications resulted in substantial improvement
573 in models of eDNA concentration across environments. Future studies on eDNA/abundance
574 relationships in nature should consider incorporating allometry, particularly when study species
575 exhibit substantial inter-population variation in size distributions. However, there is also a need
576 to validate this hypothesis in controlled experimental contexts at the level of individual
577 organisms. As a well-developed ecological theory validated by numerous empirical studies
578 (Vanni & McIntyre, 2016), the literature on the MTE represents a robust methodological

579 foundation that future studies can utilize to explore relationships between a variety of
580 environmental and ecological factors that might influence organismal production of eDNA. Such
581 studies could further improve predictive models estimating abundance from eDNA particle
582 concentration to the extent that, in some circumstances, species-specific eDNA particle
583 concentration might be a reliable ecological indicator of abundance.

584 Predictive models would need to be calibrated on a system- and species-specific basis.
585 The extent to which models for a particular species can be extended to different ecosystems or
586 geographical regions also remains unknow. Future studies employing the methodology
587 developed herein will likely need to construct models from population size/abundance estimates
588 combined with standardized size distribution data on an individual species/system basis. These
589 studies will also need to collect size distribution data, in addition to eDNA samples, to predict
590 the density or biomass of organisms in similar ecosystems that lack abundance data. Direct
591 estimates of allometric scaling coefficients for study species would also likely improve
592 predictive models, although metabolic or excretory allometric scaling coefficients estimated in
593 other empirical studies on the same (or closely related) species may represent useful starting
594 points. In the absence of any other empirical data, the general scaling coefficient predicted by the
595 MTE (0.75) may also suffice.

596 Depending on the species studied, obtaining robust population size estimates and
597 individual size distribution data to calibrate initial models can often be difficult, labour intensive,
598 and come with a substantial monetary cost. However, the benefits might be substantial – the idea
599 that future researchers or managers might be able to obtain reasonable estimates of abundance
600 from eight water samples and a small number of gill net sets is, from an ecologist's perspective,
601 exhilarating.

Acknowledgements:

We would like to thank Brent Brookes, Jacob Farkas, Tom Ridgeon, Natalie Dupont, Thaïs Bernos, Laura Bogaard, Haley Tunna, Ben Kelley, Mélia Lagacé, and Mathilde Tissier for their assistance conducting the mark-recapture experiments and collecting eDNA samples and Joanne Littlefair for her help in the laboratory. We would also like to thank Taylor Wilcox for his advice on working with the qPCR primer/probe set. This research was funded by a Fonds de recherche du Québec - Nature et technologies (FRQNT) team grant (AMD, MEC, DJF) and a Natural Sciences and Engineering Research Council of Canada (NSERC) strategic project grant (DJF, JP, AMD). DMG was funded by the NSERC Strategic Project Grant awarded to DJF and co-applicants. MCY was funded by an NSERC EcoLac post-doctoral scholarship and FRQNT post-doctoral scholarship.

613 **References**
614
615 Akaike, H. (1974). A new look at the statistical model identification. *IEEE Transactions on*
616 *Automatic Control*, *19*, 716–723.

617 Allegier, J. E., Wenger, S. J., Rosemond, A. D., Schindler, D. E., & Layman, C. A. (2015).
618 Metabolic theory and taxonomic identity predict nutrient recycling in a diverse food web.
619 *PNAS*, *112 (20)*. doi:10.1073/pnas.1420819112

620 Allen, A. P., & Gillooly, J. F. (2009). Towards an integration of ecological stoichiometry and the
621 metabolic theory of ecology to better understand nutrient cycling. *Ecology Letters*, *12*, 369–
622 384. doi:10.1111/j.1461-0248.2009.01302.x

623 Baldigo, B. P., Sporn, L. A., George, S. D., & Ball, J. A. (2017). Efficacy of environmental DNA
624 to detect and quantify brook trout populations in headwater streams of the Adirondack
625 Mountains, New York. *Transactions of the American Fisheries Society*, *146*(1), 99–111.

626 Bonar, S. A., Hubert, W. A., & Willis, D. W. (2009). *Standard methods for sampling North*
627 *American freshwater fishes*. Bethesda, Maryland: American Fisheries Society.

628 Brown, J. H., Gillooly, J. F., Allen, A. P., Savage, V. ., & West, G. B. (2004). Toward a
629 metabolic theory of ecology. *Ecology*, *85*(7), 1771–1789.

630 Burnham, K. P., & Anderson, D. R. (2002). *Model Selection and Inference: A Practical*
631 *Information-Theoretic Approach* (2nd ed.). New York: Springer-Verlag.

632 Doi, H., Uchii, K., Takahara, T., & Matsuhashi, S. (2015). Use of Droplet Digital PCR for
633 Estimation of Fish Abundance and Biomass in Environmental DNA Surveys. *PLoS ONE*,
634 1–11. doi:10.1371/journal.pone.0122763

635 Donald, D. B., Anderson, R. S., Mayhood, D. W., Anderson, R. S., & Correlations, D. W. M.
636 (1980). Correlations Between Brook Trout Growth and Environmental Variables for
637 Mountain Lakes in Alberta. *Transactions of the American Fisheries Society*, *109*(October),
638 603–610. doi:10.1577/1548-8659(1980)109<603

639 Eichmiller, J. J., Miller, L. M., & Sorensen, P. W. (2016). Optimizing techniques to capture and
640 extract environmental DNA for detection and quantification of fish. *Molecular Ecology*
641 *Resources*, *16*, 56–68. doi:10.1111/1755-0998.12421

642 Glazier, D. S. (2005). Beyond the '3/4-power law': variation in the intra- and interspecific
643 scaling of metabolic rate in animals. *Biological Reviews*, *80*, 611–662.
644 doi:10.1017/S1464793105006834

645 Goldberg, C. S., Strickler, K. M., & Pilliod, D. S. (2015). Moving environmental DNA methods
646 from concept to practice for monitoring aquatic macroorganisms. *Biological Conservation*,
647 *183*, 1–3. doi:10.1016/j.biocon.2014.11.040

648 Guernon, S., Yates, M. C., Fraser, D. J., & Derry, A. M. (2018). The co-evolution of adult body
649 mass and excretion rate between genetically size-divergent brook trout populations. *CJFAS*,
650 *Online*. doi:http://dx.doi.org/10.1007/s00787-010-0141-5

651 Hartman, K. J., & Cox, M. (2008). Refinement and Testing of a Brook Trout Bioenergetics

652 Model. *Transactions of the American Fisheries Society*, *137*(June 2014), 357–363.
653 doi:10.1577/T05-243.1

654 Hubert, W. ., Pope, K. L., & Dettmers, J. M. (2012). Passive Capture Techniques. In A. V. Zale,
655 D. L. Parrish, & T. . Sutton (Eds.), *Fisheries Techniques* (3rd ed.). Bethesda, Maryland:
656 American Fisheries Society.

657 Id, Y. M., Wong, M. K., Kanbe, T., Araki, H., Kashiwabara, T., Ijichi, M., … Hyodo, S. (2019).
658 Spatiotemporal distribution of juvenile chum salmon in Otsuchi Bay, Iwate, Japan, inferred
659 from environmental DNA. *PLoS ONE*, 1–22. Retrieved from
660 https://doi.org/10.1371/journal.pone.0222052 September

661 Immell, D., & Anthony, R. G. (2008). Estimation of Black Bear Abundance Using a Discrete
662 DNA Sampling Device. *The Journal of Wildlife Management*, *72*(1), 324–330.
663 doi:10.2193/2006-297

664 Isaac, N. J. ., & Carbone, C. (2010). Why are metabolic scaling exponents so controversial?
665 Quantifying variance and testing hypotheses. *Ecology Letters*, *13*, 728–735.
666 doi:10.1111/j.1461-0248.2010.01461.x

667 Jamieson, I. G., & Allendorf, F. W. (2012). How does the 50/500 rule apply to MVPs? *Trends in*
668 *Ecology and Evolution*, *27*(10), 580–584. doi:10.1016/j.tree.2012.07.001

669 Jo, T., Murakami, H., Yamamoto, S., Masuda, R., & Minamoto, T. (2019). Effect of water
670 temperature and fish biomass on environmental DNA shedding, degradation, and size
671 distribution. *Ecology and Evolution*, (September 2018), 1–12. doi:10.1002/ece3.4802

672 Johnson, L. (1983). Homeostatic Characteristics of Single Species Fish Stocks in Arctic Lakes.
673 *Canadian Journal of Fisheries and Aquatic Sciences*, *40*(96393), 987–1024.

674 Klobucar, S. L., Rodgers, T. W., & Budy, P. (2017). At the forefront: evidence of the
675 applicability of using environmental DNA to quantify the abundance of fish populations in
676 natural lentic waters with additional sampling considerations. *Canadian Journal of*
677 *Fisheries and Aquatic Sciences*, *74*, 2030–2034.

678 Klymus, K. E., Richter, C. A., Chapman, D. C., & Paukert, C. (2015). Quantification of eDNA
679 shedding rates from invasive bighead carp Hypophthalmichthys nobilis and silver carp
680 Hypophthalmichthys molitrix. *Biological Conservation*, *183*, 77–84.
681 doi:10.1016/j.biocon.2014.11.020

682 Krebs, C. J. (2009). *Ecology: The experimental analysis of distribution and abundance.* (6th ed.).
683 San Francisco, CA: Pearson Benjamin Cummings.

684 Lacoursière-Roussel, A., Côté, G., Leclerc, V., Bernatchez, L., & Cadotte, M. (2016).
685 Quantifying relative fish abundance with eDNA: a promising tool for fisheries management.
686 *Journal of Applied Ecology*, *53*(4), 1148–1157. doi:10.1111/1365-2664.12598

687 Lacoursière-Roussel, A., Rosabal, M., & Bernatchez, L. (2016). Estimating fish abundance and
688 biomass from eDNA concentrations: variability among capture methods and environmental
689 conditions. *Molecular Ecology Resources*, *16*, 1401–1414. doi:10.1111/1755-0998.12522

690 Levi, T., Allen, J. M., Bell, D., Joyce, J., Russell, J. R., David, A., … Yu, D. W. (2019).

691 Environmental DNA for the enumeration and management of Pacific salmon. *Molecular*
692 *Ecology Resources*, *19*, 597–608.

693 Luikart, G., Ryman, N., Tallmon, D. A., Schwartz, M. K., & Allendorf, F. W. (2010). Estimation
694 of census and effective population sizes: The increasing usefulness of DNA-based
695 approaches. *Conservation Genetics*, *11*(2), 355–373. doi:10.1007/s10592-010-0050-7

696 Maruyama, A., Nakamura, K., Yamanaka, H., Kondoh, M., & Minamoto, T. (2014). The release
697 rate of environmental DNA from juvenile and adult fish. *PLoS ONE*, *9*(12), 1–13.
698 doi:10.1371/journal.pone.0114639

699 McNicol, R. E., Scherer, E., & Murkin, E. J. (1985). Quantitative field investigations of feeding
700 and territorial behaviour of young- of-the-year brook charr, Salvelinus fontinalis.
701 *Environmental Biology of Fishes*, *12*(3), 219–229.

702 Millien, V., Lyons, K., Olson, L., Smith, F. A., Wilson, A. B., & Yom-Tov, Y. (2006). Ecotypic
703 variation in the context of global climate change: revisiting the rules. *Ecology Letters*, *9*,
704 853–869. doi:10.1111/j.1461-0248.2006.00928.x

705 Mizumoto, H., Urabe, H., Kanbe, T., Fukushima, M., & Araki, H. (2017). Establishing an
706 environmental DNA method to detect and estimate the biomass of Sakhalin taimen, a
707 critically endangered Asian salmonid. *Limnology*, *19*, 219–227. doi:10.1007/s10201-017-
708 0535-x

709 Morgan, G. E. (2002). *Manual of instructions - fall walleye index netting (FWIN)*. Retrieved
710 from https://www.ontario.ca/page/fall-walleye-index-netting-instructions#section-8

711 Nevers, M. B., Byappanahalli, M. N., Morris, C. C., Shively, D., Przybyla-kelly, K., Spoljaric,
712 A. M., … Roseman, E. F. (2018). Environmental DNA (eDNA): A tool for quantifying the
713 abundant but elusive round goby (Neogobius melanostomus). *PloS One*, 1–22.
714 doi:10.5066/F7GH9H6F.Funding

715 Ogle, D. H. (2016). *Introductory Fisheries Analyses with R* (1st ed.). Boca Raton: CRC Press.

716 Ovenden, J. R., Blower, D. C., Dudgeon, C. L., Jones, A. T., Buckworth, R. C., Leigh, G. M., …
717 Bennett, M. B. (2016). Can genetic estimates of population size contribute to fisheries stock
718 assessements? *Journal of Fish Biology*, 1–14. doi:10.1111/jfb.13129

719 Pilliod, D. S., Goldberg, C. S., Arkle, R. S., & Waits, L. P. (2013). Estimating occupancy and
720 abundance of stream amphibians using environmental DNA from filtered water samples.
721 *Canadian Journal of Fisheries and Aquatic Sciences*, *1130*(January), 1123–1130.

722 Pilliod, D. S., Goldberg, C. S., Arkle, R. S., & Waits, L. P. (2014). Factors Influencing Detection
723 of eDNA from a Stream-dwelling Amphibian Authors. *Molecular Ecology Resources*, *1*,
724 109–116. doi:10.1111/1755-0998.12159

725 Poisot, T. (2011). The digitize package: extracting numerical data from scatterplots. *The R*
726 *Journal*, *3*(1), 25–26.

727 Post, J. R., Parkinson, E. A., & Johnston, N. T. (1999). Density-dependent processes in structures
728 fish populations: interaction strengths in whole-lake experiments. *Ecological Monographs*,
729 *69*(2), 155–175.

R Development Core Team. (2017). R: a language and environment for statistical computing. *R Foundation for Statistical Computing Vienna Austria*, *0*, {ISBN} 3-900051-07-0. doi:10.1038/sj.hdy.6800737

Rose, G. A., & Kulka, D. W. (1999). Hyperaggregation of fish and fisheries: how catch-per-unit-effort increased as the northern cod (Gadus morhua) declined. *Canadian Journal of Fisheries and Aquatic Sciences*, *56*, 118–127.

Schaus, M. H., Godwin, W., Battoe, L., Coveney, M., Lowe, E., Roth, R., … Zimmerman, A. (2010). Impact of the removal of gizzard shad (Dorosoma cepedianum) on nutrient cycles in Lake Apopka, Florida. *Freshwater Biology*, *55*, 2401–2413. doi:10.1111/j.1365-2427.2010.02440.x

Schindler, D. E., & Eby, L. A. (1997). Stoichiometry of fishes and their prey: implications for nutrient recycling. *Ecology*, *78*(6), 1816–1831.

Schmelzle, M. C., & Kinziger, A. P. (2016). Using occupancy modelling to compare environmental DNA to traditional field methods for regional-scale monitoring of an endangered aquatic species. *Molecular Ecology Resources*, *16*, 895–908. doi:10.1111/1755-0998.12501

Schnabel, Z. E. (1938). The Estimation of the Total Fish Population of a Lake. *The American Mathematical Monthly*, *46*, 348–352. doi:10.1080/00029890.1938.11990818

Schwarz, C. J., & Seber, G. A. F. (1999). A review of estimating animal abundance III. *Statistical Science*, *14*, 1–126.

Sebens, K. P. (1987). The ecology of indeterminate growth in animals. *Annual Review of Ecology and Systematics*, *18*, 371–407.

Seber, G. A. F. (1986). A Review of Estimating Animal Abundance. *Biometrics*, *42*(2), 267–292.

Seber, G. A. F. (2002). *The Estimation of Animal Abundance and Related Parameters* (2nd ed.). New Jersey: Blackburn Publishing.

Shea, B. O., Fryer, R. J., Pert, C. C., & Bricknell, I. R. (2006). Determination of the surface area of a fish. *Journal of Fish Diseases*, *29*, 437–440.

Stewart, K. A. (2019). Understanding the effects of biotic and abiotic factors on sources of aquatic environmental DNA Understanding the effects of biotic and abiotic factors. *Biodiversity and Conservation*, (February). doi:10.1007/s10531-019-01709-8

Stitt, B, P. C. (2018). *2018 summary report for the chemical removal of brook trout from Hidden Lake, Upper Corral Creek and Tributaries - Draft report.*

Sullivan, Sierra, P. C. (2017). *Saving wild trout: Upper Corral Creek and Hidden Lake brook trout removal and Westslope Cutthroat trout reintroduction - Banff National Park, Draft Report*.

Takahara, T., Minamoto, T., Yamanaka, H., Doi, H., & Kawabata, Z. (2012). Estimation of Fish Biomass Using Environmental DNA. *PLoS ONE*, *7*(4), 3–10. doi:10.1371/journal.pone.0035868

768 Takeuchi, A., Iijima, T., Kakuzen, W., Watanab, S., & Yamada, Y. (2019). Release of eDNA by
769 different life history stages and during spawning activities of laboratory-reared Japanese
770 eels for interpretation of oceanic survey data. *Scientific Reports*, *9*(April), 1–9.
771 doi:10.1038/s41598-019-42641-9

772 Thomsen, P. F., Kielgast, J. O. S., Iversen, L. L., Wiuf, C., Rasmussen, M., Thomas, M., …
773 Willerslev, E. (2012). Monitoring endangered freshwater biodiversity using environmental
774 DNA. *Molecular Ecology*, *21*, 2565–2573. doi:10.1111/j.1365-294X.2011.05418.x

775 Tillotson, M. D., Kelly, R. P., Duda, J., Hoy, M., Kralj, J., & Quinn, T. P. (2018). Concentrations
776 of environmental DNA (eDNA) reflect spawning salmon abundance at fine spatial and
777 temporal scales. *Biological Conservation*, *220*(February), 1–11.
778 doi:10.1016/j.biocon.2018.01.030

779 Vanni, M. J., & McIntyre, P. B. (2016). Predicting nutrient excretion of aquatic animals with
780 metabolic ecology and ecological stoichiometry: A global synthesis. *Ecology*, *97*(12),
781 3460–3471. doi:10.1002/ecy.1582

782 Ward, H. G. M., Askey, P. J., Post, J. R., Varkey, D. A., & Mcallister, M. K. (2012). Basin
783 characteristics and temperature improve abundance estimates from standard index netting of
784 rainbow trout (Oncorhynchus mykiss) in small lakes. *Fisheries Research*, *131–133*, 52–59.
785 doi:10.1016/j.fishres.2012.07.011

786 Wilcox, T. M., Mckelvey, K. S., Young, M. K., Jane, S. F., Lowe, W. H., Whiteley, A. R., &
787 Schwartz, M. K. (2013). Robust Detection of Rare Species Using Environmental DNA: The
788 Importance of Primer Specificity. *PLoS ONE*, *8*(3). doi:10.1371/journal.pone.0059520

789 Wilcox, T. M., Mckelvey, K. S., Young, M. K., Sepulveda, A. J., Shepard, B. B., Jane, S. F., …
790 Schwartz, M. K. (2016). Understanding environmental DNA detection probabilities : A case
791 study using a stream-dwelling char Salvelinus fontinalis. *Biological Conservation*, *194*,
792 209–216. doi:10.1016/j.biocon.2015.12.023

793 Yates, M. C., Bernos, T. A., & Fraser, D. J. (2017). A critical assessment of estimating census
794 population size from genetic population size (or vice versa) in three fishes. *Evolutionary*
795 *Applications*, *10*(9). doi:10.1111/eva.12496

796 Yates, M. C., Fraser, D. J., & Derry, A. M. (2019). Meta-analysis supports further refinement of
797 eDNA for monitoring aquatic species-specific abundance in nature. *Environmental DNA*,
798 *1*(January), 5–13. doi:10.1002/edn3.7

799

800 **Data Accessibility Statement:**

801 eDNA particle concentration data for each lake will be deposited in the Dryad Digital Repository

802 upon acceptance.

Author contributions

MCY collected eDNA samples and analyzed eDNA data. DG collected and analyzed mark-recapture and size structure data. Statistical analyses were conducted by MCY. MCY wrote the first draft of the manuscript, and all authors contributed substantially to subsequent drafts.

807 **Tables**

808 Table 1: Size structure gill net effort and fyking (mark-recapture) effort. SS refers to size
809 structure assessment, percent SS refers to the proportion of population harvested during size
810 structure assessment.
811

Site	SS Samples	Percent SS	SS CPUE	Mark/Recapture days	Total Marks Applied
Cobb	104	0.72	7	20	24
Mud	84	0.10	42	20	364
Olive	160	0.09	53	21	307
Ross	128	0.09	64	19	571
Temple	165	0.10	41	25	409
Dog	187	0.06	94	30	617
Helen	41	0.07	41	12	172
Margaret	171	0.08	43	23	414
McNair	27	0.13	27	14	118

812

813

814 Table 2: Density metric estimates for each population. N = population size, ASM =
815 allometrically scaled mass. 95% confidence intervals for 'N' are given in brackets.
816

Site	N	Ha	Mean Ind. Mass (g)	Fish/ha	Kg/ha	ASM/ha	eDNA (copies/L)
Cobb	145 (94, 237)	2.3	404.8	63	25.7	5663	592.2
Dog	3266 (2715, 4097	11.5	184.8	284	52.5	13962	5131.1
Helen	557 (420, 755)	2.5	83.9	225	18.8	6187	2445.9
Margaret	2017 (1638, 2623)	18.0	112.3	112	12.6	3707	1240.4
McNair	201 (158, 276)	1.7	137.3	121	16.6	4736	3050.5
Mud	860 (733, 1040)	7.2	141.9	119	17.0	4587	1138.7
Olive	1877 (1459, 2628)	1.7	43.1	1131	48.8	18601	7805.1
Ross	1392 (1211, 1635)	6.6	82.5	211	17.4	5559	917.4
Temple	1655 (1369, 2090)	3.3	51.1	509	26.1	9587	2076.5

817

818

819 Table 3: Lake zone area and corresponding eDNA concentrations.

Site	Pelagic area (ha)	Littoral area (ha)	Pelagic eDNA (copies/L)	Littoral eDNA (Copies/L)	Weighted Mean eDNA (Copies/L)
Cobb	1.0	1.3	253.8	854.6	592.2
Dog	8.5	3.1	3447.1	9796.7	5131.1
Helen	1.2	1.3	1342.4	3514.4	2445.9
Margaret	14.4	3.6	791.9	3034.1	1240.4
McNair	0.7	1.0	2395.4	3505.0	3050.5
Mud	4.7	2.6	621.3	2280.1	1138.7
Olive	0.5	1.2	8084.6	7684.7	7805.1
Ross	4.6	2.0	790.5	1209.8	917.4
Temple	1.6	1.7	1940.8	2200.2	2076.5
Hidden	11.8	2.6	342.0	2652.9	847.2

820

821

822 Table 4: Model results evaluating the relationship between eDNA particle concentration and
823 density (fish/ha), biomass (kg/ha), allometrically scaled mass (ASM/ha), and CPUE.
824

Model	F-value	P-value	Adj. R^2	Log Likelihood	AIC	ΔAIC
Density	$12.37_{(1,7)}$	0.010	0.59	-77.78	161.6	5.7
Biomass	$14.76_{(1,7)}$	0.006	0.63	-77.26	160.5	4.6
ASM	$29.4_{(1,7)}$	0.001	0.78	-74.95	155.9	-
CPUE	$1.92_{(1,7)}$	0.208	0.10	-81.27	168.5	12.6

825

826

827 **Figure Captions**
828
829 Figure 1: Lake size structure distributions (g) obtained from standardized gill net sets for the nine
830 study lakes.
831
832 Figure 2: Correlation between weighted mean lake brook trout eDNA particle concentration and
833 three metrics of abundance in the nine study lakes: (a) individual density (individuals/ha, R^2 =
834 0.59), (b) biomass density (kg/ha, R^2 = 0.63), and (c) allometrically scaled mass (ASM/ha, R^2 =
835 0.78) (n = 9).
836
837 Figure 3: Predicting allometrically scaled mass (ASM/ha) for Hidden Lake based on eDNA
838 particle concentration. Black dots represent values for the nine study lakes, gray circle represents
839 the ASM/ha point estimate for Hidden Lake. Error bars represent 95% prediction intervals (n =
840 9).
841
842 Figure 4: AIC values for models correlating brook trout eDNA and allometrically scaled mass
843 (ASM), utilizing allometric scaling coefficients ranging from 0.00 (corresponding to individual
844 density) to 1.0 (corresponding to biomass density). Horizontal black bars and dotted lines denote
845 range of models with $\Delta AIC < 2$ relative to the 'optimal' scaling coefficient (0.72).
846
847 Figure S1: Map of the nine study lakes located in Alberta and British Columbia, Canada.
848
849 Figure S2: Timing of sampling activities in 2018.
850
851 Figure S3: Relationship between catch-per-unit-effort (CPUE) of a large and small gill net and
852 individual density (fish/ha) for the nine study lakes (adjusted $R^2 < 0$) (n = 9).
853
854 Figure S4: Relationship between brook trout eDNA particle concentration and catch-per-unit-
855 effort (CPUE) of a large and small gill net for the nine study lakes ($R^2 = 0.10$).

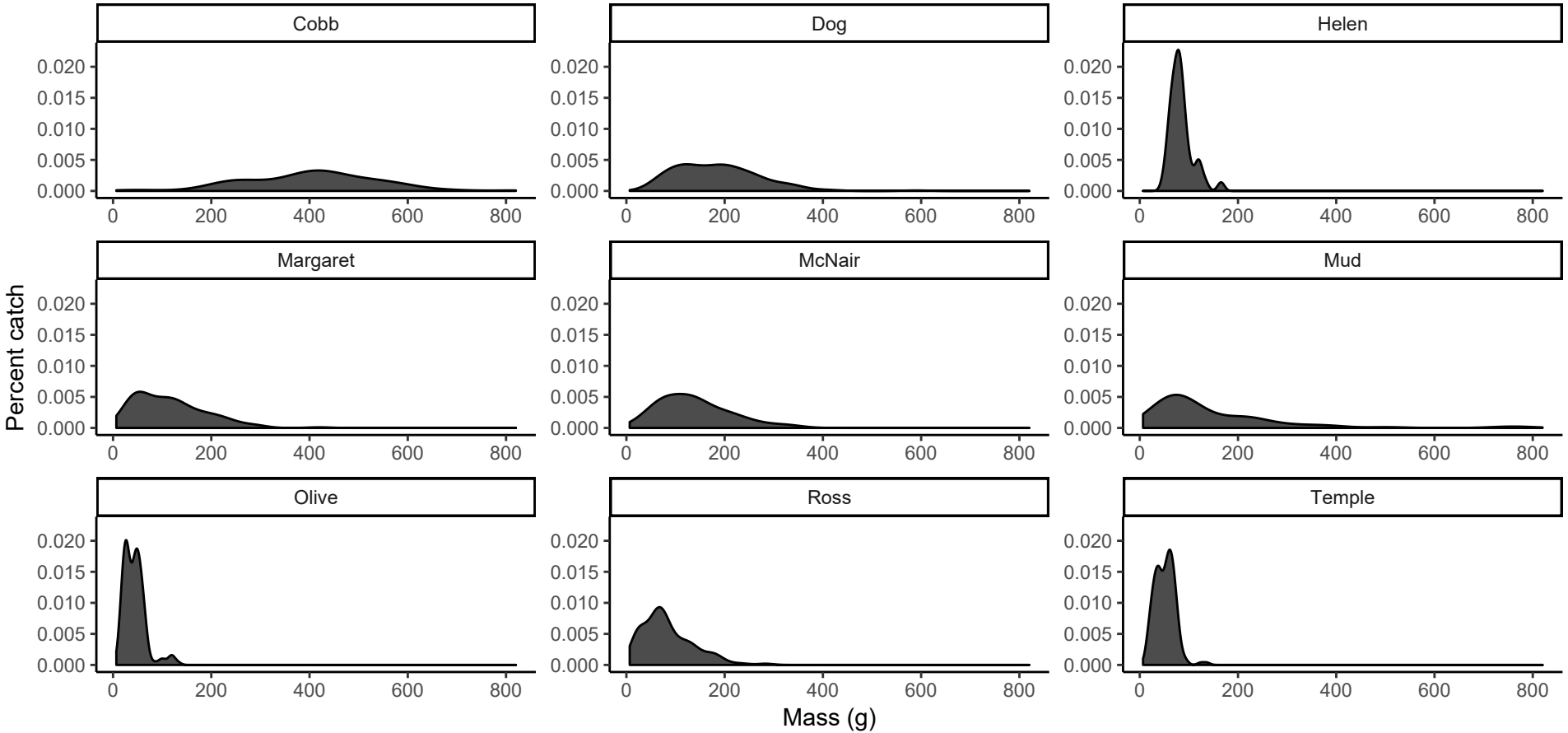
Cobb
Dog
Helen
Margaret
McNair
Mud
Olive
Ross
Temple
Percent catch
Mass (g)
0.020
0.015
0.010
0.005
0.000
0
200
400
600
800

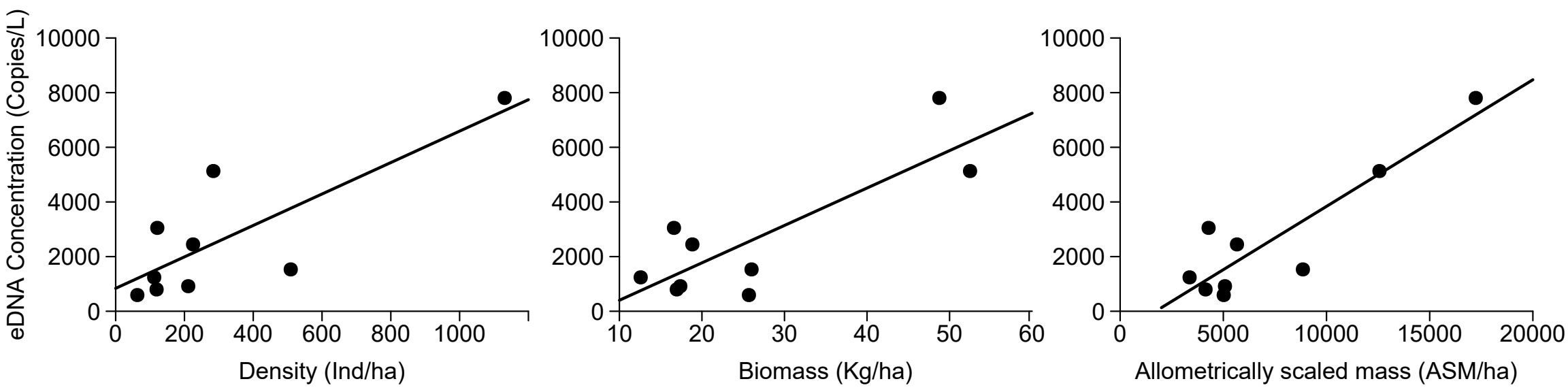
eDNA Concentration (Copies/L)
10000
8000
6000
4000
2000
0
0
200
400
600
800
1000
Density (Ind/ha)
10000
8000
6000
4000
2000
0
10
20
30
40
50
60
Biomass (Kg/ha)
10000
8000
6000
4000
2000
0
0
5000
10000
15000
20000
Allometrically scaled mass (ASM/ha)

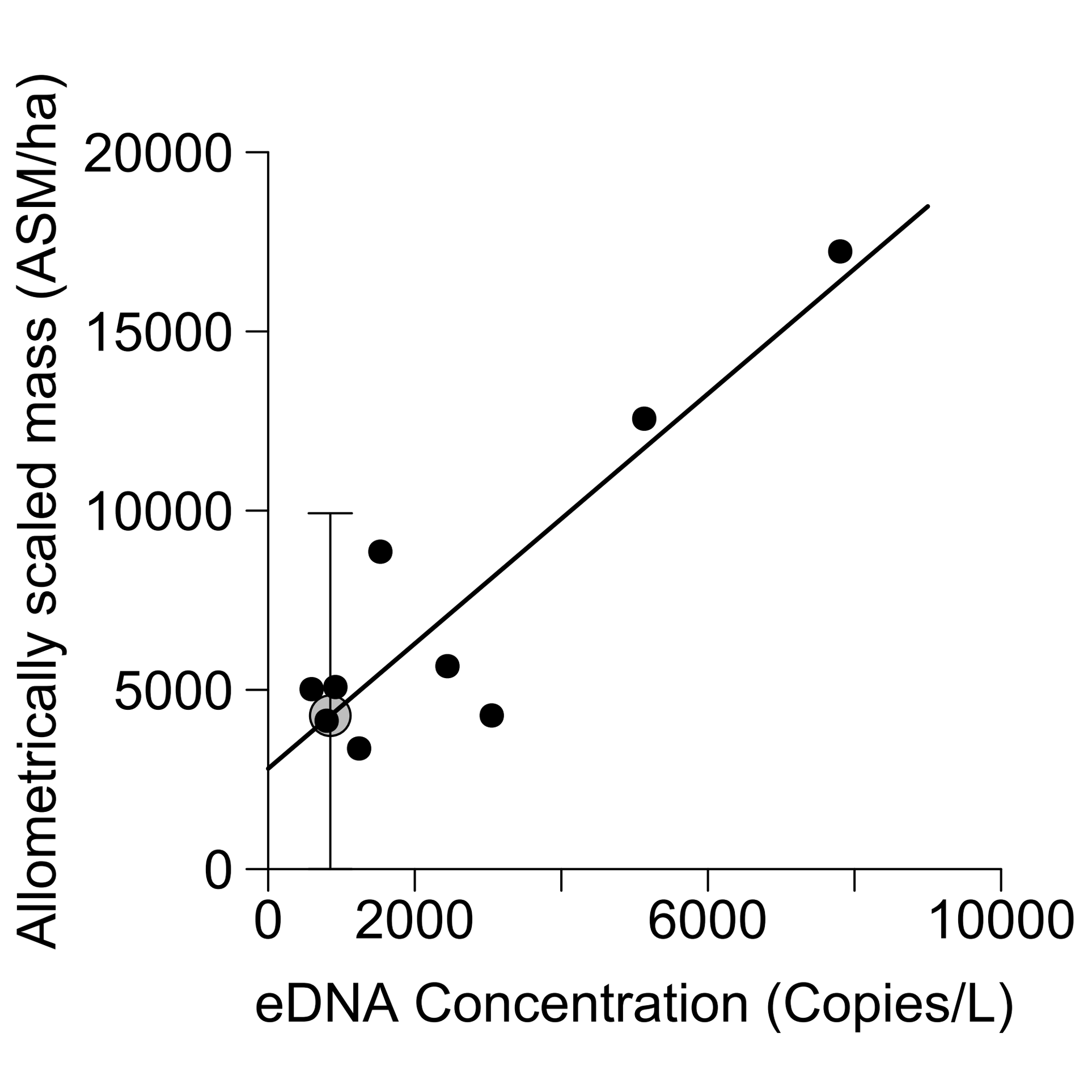
Allometrically scaled mass (ASM/ha)
20000
15000
10000
5000
0
0
2000
6000
10000
eDNA Concentration (Copies/L)

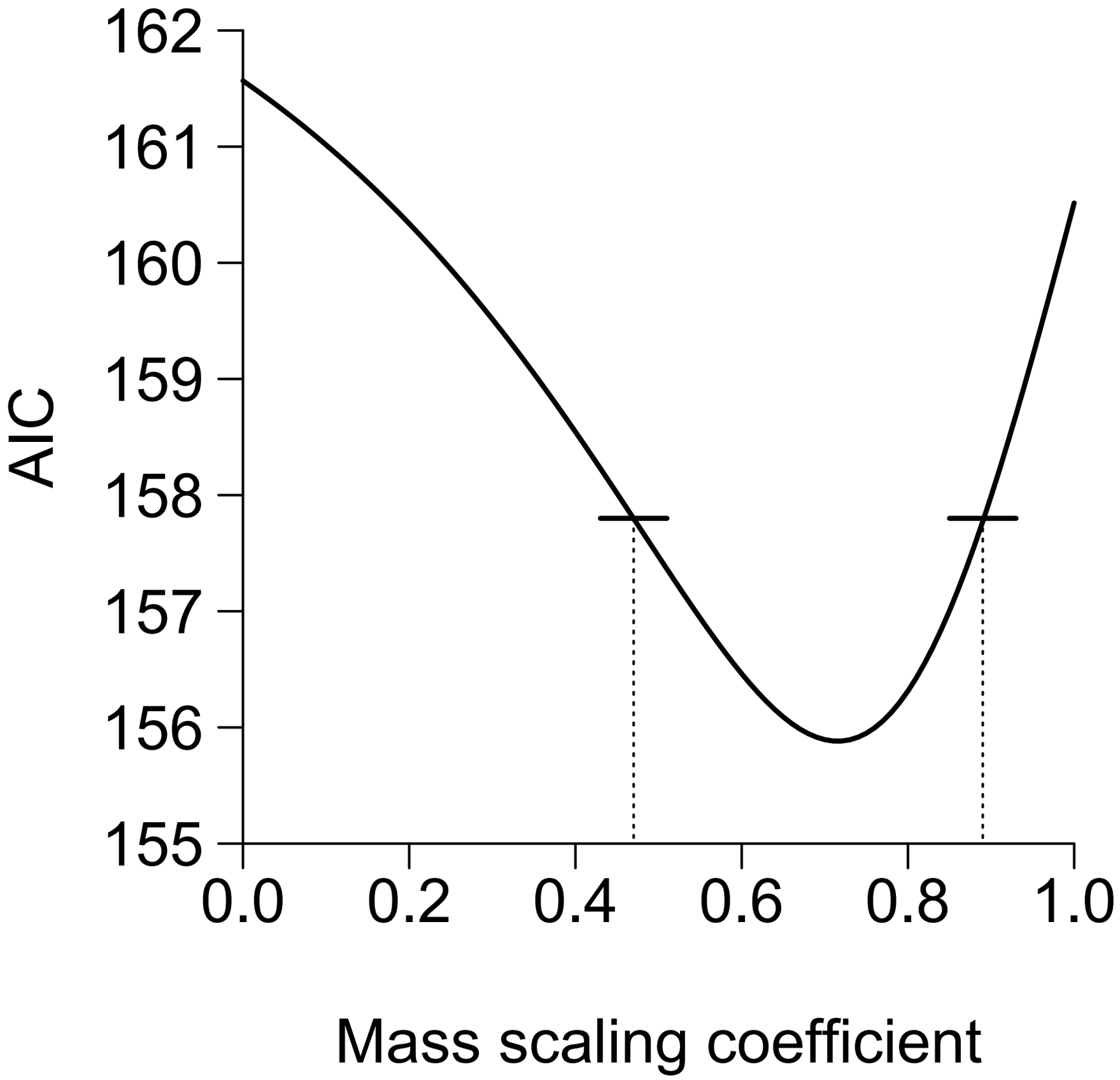
AIC
162
161
160
159
158
157
156
155
0.0
0.2
0.4
0.6
0.8
1.0
Mass scaling coefficient